

## **HYBRID-SURROGATE-MODEL-BASED EFFICIENT GLOBAL OPTIMIZATION FOR HIGH-DIMENSIONAL ANTENNA DESIGN**

**L.-L. Chen<sup>\*</sup>, C. Liao, W.-B. Lin, L. Chang, and X.-M. Zhong**

Institute of Electromagnetics, Southwest Jiaotong University, Chengdu, Sichuan 610031, China

**Abstract**—Efficient global optimization has been extensively used in problems with expensive cost functions. However, this method is not suitable for high-dimensional problems. In this paper, the radial basis function network is introduced into the efficient global optimization, to avoid local optima and achieve a fast convergence for high-dimensional optimization. Our algorithm is applied to a 12-dimensional optimization of a transmitting antenna. Compared to the genetic-algorithm-based efficient global optimization and the differential evolution strategy, our algorithm converges to the global optimal value more efficiently.

### **1. INTRODUCTION**

Conventional efficient global optimization (EGO) which employs the Kriging model is an efficient evolutionary algorithm for the low-dimensional optimization problems [1]. In comparison with the population-based optimization techniques, such as the genetic algorithm (GA) [2–5], particle swarm optimization (PSO) [6–14] and differential evolution strategy (DES) [15–21], the EGO requires fewer function evaluations to obtain the global optimum [22–27]. However, it is difficult for the conventional EGO to avoid falling into local optima when the dimensions of optimization increase [24, 25]. In order to overcome this difficulty, some improved EGO algorithms have been proposed for high-dimensional problems, e.g., the Taguchi's-method-based EGO [26] and the GA-based EGO [27]. However, the convergence rates of these methods remain to be improved.

---

*Received 12 December 2011, Accepted 6 January 2012, Scheduled 12 January 2012*

\* Corresponding author: Ling-Lu Chen (zjwycl@163.com).

An effective approach for fast convergence is to add new sampling points around the optimum of the surrogate model and the sparse region in the design space simultaneously [28, 29]. In this paper, we use the Kriging model and the radial basis function (RBF) network to determine the new sampling points. Numerical examples show that the global optimum can be found with a small number of function evaluations via this sampling strategy.

The remainder of this paper is organized as follows. Section 2 introduces the conventional EGO algorithm briefly. In Section 3 the RBF network and the density function [30] for the sparse region searching are described, and the new algorithm is presented. Section 4 demonstrates the advantages of our algorithm with a 12-dimensional optimization of a transmitting antenna [31]. Conclusions are given in Section 5.

## 2. THE CONVENTIONAL EGO ALGORITHM

The detailed descriptions of the conventional EGO algorithm can be found in [1], and we only present its main ideas here. The procedure of the conventional EGO is shown in Fig. 1.

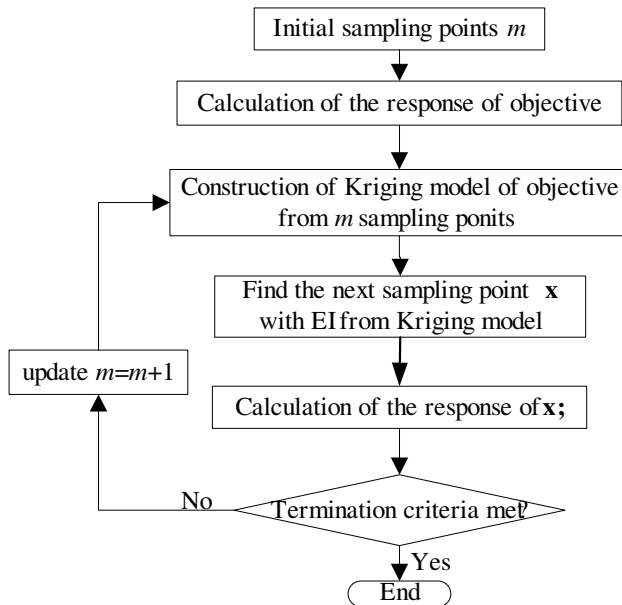


**Figure 1.** The flow chart of the conventional EGO algorithm.

The EGO algorithm begins by fitting a surrogate model to the data which are obtained by evaluating the cost function at a limited number of sampling points. The initial sampling points are chosen randomly or by some space-filling techniques, such as the Latin hypercube, orthogonal array and uniform design [32]. The surrogate model is then refined with only a few of additional function evaluations. Finally, the global optimum in the surrogate model can be obtained.

The surrogate model employed in the EGO algorithm [1, 22-27] is the Kriging model, which can be written as

$$f_k(\mathbf{x}) = \mu + \mathbf{r}'\mathbf{R}^{-1}(\mathbf{y} - \mathbf{I}\mu), \quad (1)$$

where  $f_k(\mathbf{x})$  represents the predicted value by the Kriging model.  $\mu = (\mathbf{I}'\mathbf{R}^{-1}\mathbf{y})/(\mathbf{I}'\mathbf{R}^{-1}\mathbf{I})$  denotes the mean of the function with  $\mathbf{R}$  being a  $m \times m$  matrix whose  $(i, j)$  entry is  $Corr(\mathbf{x}_i, \mathbf{x}_j)$ . Here  $\mathbf{x}_i$  is the  $i$ -th sampling point.  $\mathbf{y} = [y_1 \ y_2 \ \dots \ y_m]$  represents the responses which are obtained by evaluating the cost function at the sampled points.  $\mathbf{r}' = [Corr(\mathbf{x}, \mathbf{x}_1) \ \dots \ Corr(\mathbf{x}, \mathbf{x}_m)]$  is the correlation between the point  $\mathbf{x}$  and all previously sampled points.

The expected improvement (EI) in the EGO can be expressed as

$$EI(\mathbf{x}) = [y_{\min} - f_k(\mathbf{x})] \varphi \left[ \frac{y_{\min} - f_k(\mathbf{x})}{s(\mathbf{x})} \right] + s(\mathbf{x}) \Phi \left[ \frac{y_{\min} - f_k(\mathbf{x})}{s(\mathbf{x})} \right], \quad (2)$$

where  $y_{\min} = \min[y_1 \ y_2 \ \dots \ y_m]$  denotes the current best response value,  $\varphi(u)$  and  $\Phi(u)$  are the normal probability density function and the probability distribution function with the standard deviation  $s(\mathbf{x})$  respectively.

The location of the maximum value of EI in the design space is used as the new sampling point which needs to be evaluated. The balance between the local and global searches of the EGO can be achieved by the evaluation of EI [24].

The stopping rule of the EGO algorithm can be chosen such that the absolute value of EI at the next sampling point is less than 1% of  $y_{\min}$  [1], or a maximum number of iteration is reached.

### 3. THE HYBRID-SURROGATE-MODEL-BASED EGO ALGORITHM

The most consuming part for the EGO algorithm is to refine the surrogate model. Since the number of sampling points in constructing the surrogate model in the EGO increases significantly with the dimension number, the superiority of the conventional EGO algorithm will be lost for the high-dimensional problems. One efficient method to construct the surrogate model is simultaneously adding the new

sampling points around the optimum of the surrogate model and the sparse region in the design space [28, 29]. In this paper, the hybrid surrogate model consists of the RBF network and Kriging model is used to implement this sampling strategy for the fast convergence of EGO.

### 3.1. RBF Network

An RBF network is a three-layer feed-forward network. The output of the network  $f_R(\mathbf{x})$  is given by

$$f_R(\mathbf{x}) = \sum_{i=1}^m w_i h_i(\mathbf{x}), \quad (3)$$

where  $m$  represents the number of sampling points,  $h_i(\mathbf{x})$  and  $w_i$  are the  $i$ -th basis function and its weight. The basis function is chosen as

$$h_i(\mathbf{x}) = \exp\left(-\frac{(\mathbf{x} - \mathbf{x}_i)'(\mathbf{x} - \mathbf{x}_i)}{r_i^2}\right), \quad (4)$$

where  $r_i$  is the width of the  $i$ -th basis function. The learning of the RBF network is usually accomplished by solving

$$E = \sum_{i=1}^m (y_i - f_R(\mathbf{x}_i))^2 + \sum_{i=1}^m \lambda_i w_i^2 \rightarrow \min, \quad (5)$$

where  $y_i$  is obtained by evaluating the cost function at the sampled point  $\mathbf{x}_i$  and the second term is introduced for the purpose of regularization. It is recommended that  $\lambda_i$  in Eq. (5) has a small value (e.g.,  $\lambda_i = 1.0 \times 10^{-3}$ ). Thus, the learning of the RBF network is equivalent to finding the weight vector [30]

$$\mathbf{w} = (\mathbf{H}'\mathbf{H} + \mathbf{\Lambda})^{-1}\mathbf{H}'\mathbf{y}, \quad (6)$$

where  $\mathbf{H}$ ,  $\mathbf{\Lambda}$  and  $\mathbf{y}$  are given by

$$\mathbf{H} = \begin{bmatrix} h_1(\mathbf{x}_1) & h_2(\mathbf{x}_1) & \cdots & h_m(\mathbf{x}_1) \\ h_1(\mathbf{x}_2) & h_2(\mathbf{x}_2) & \cdots & h_m(\mathbf{x}_2) \\ \vdots & \vdots & \ddots & \vdots \\ h_1(\mathbf{x}_m) & h_2(\mathbf{x}_m) & \cdots & h_m(\mathbf{x}_m) \end{bmatrix} \quad (7)$$

$$\mathbf{\Lambda} = \begin{bmatrix} \lambda_1 & 0 & \cdots & 0 \\ 0 & \lambda_2 & \cdots & 0 \\ \vdots & \vdots & \ddots & \vdots \\ 0 & 0 & \cdots & \lambda_m \end{bmatrix} \quad (8)$$

$$\mathbf{y} = (y_1 \ y_2 \ \cdots \ y_m)'. \quad (9)$$

The RBF network can be incorporated into EGO easily, since the sampling point is added gradually and the additional learning reduced to the incremental calculation of the matrix inversion in the EGO. The detailed procedure can be found in [33].

### 3.2. Density Function

The introduction of the density function is to discover a sparse region in the design space. The basic concept of the construction of a density function using the RBF network is very simple.

We set the output of density function  $y_i^D$  at the sampled point  $\mathbf{x}_i$  as “+1”, i.e.,  $\mathbf{y}^D = (1 \ 1 \ \dots \ 1)'_{m \times 1}$ . The weight vector  $\mathbf{w}^D$  of density function  $D(\mathbf{x})$  is calculated as  $\mathbf{w}^D = (\mathbf{H}'\mathbf{H} + \mathbf{\Lambda})^{-1}\mathbf{H}'\mathbf{y}^D$ , and the density function  $D(\mathbf{x})$  is written as

$$D(\mathbf{x}) = \sum_{i=1}^m w_i^D h_i(\mathbf{x}). \quad (10)$$

The point at which the density function  $D(\mathbf{x})$  is minimum will be taken as the new sampling point. It is expected that the addition of the new sampling points in the sparse region will prevent the EGO falling into the local optima.

### 3.3. Algorithm for EGO using Hybrid Surrogate Model

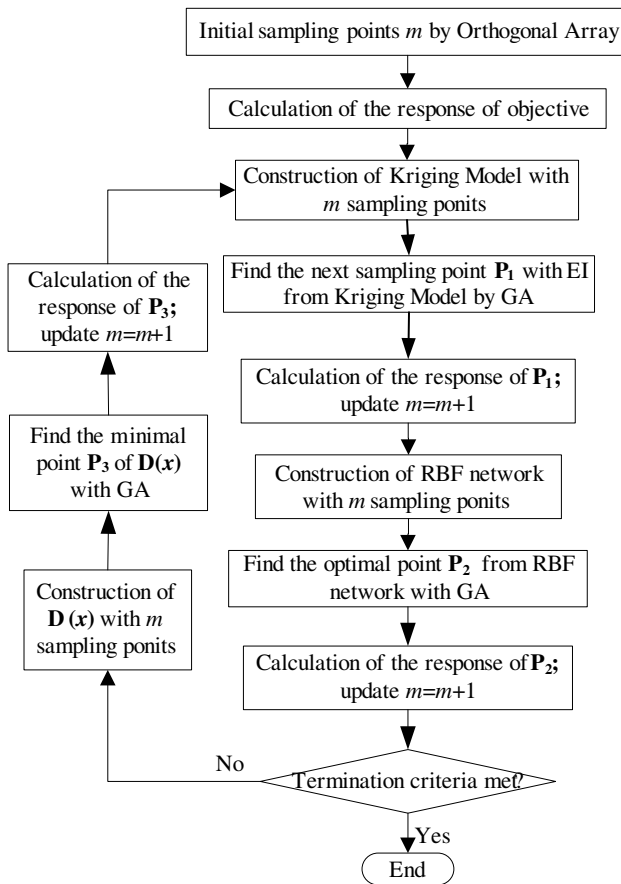
As the surrogate models with large dimensions are not accurate at the beginning of the optimization, one can increase the diversity of sampling and expand the search domain by the combination of different surrogate models. Therefore, the RBF network and the Kriging model are employed alternatively in the iterations in optimization procedure.

Figure 2 shows the details for the hybrid-surrogate-model-based EGO algorithm (HSM-based EGO). The orthogonal array (OA) is introduced to determine the initial sampling points [32]. It provides a sparse and balanced design for any projection into  $k$  dimensions in the optimization problem. The number of initial samples  $m$  is determined by the strength of the array and the number of levels. The responses at these sampling points are calculated by the cost function.

A Kriging model is constructed from  $m$  sampling points, and the first new sampling point  $\mathbf{P}_1$  is generated by searching the maximum value of EI in the design space. This is a quasi-global search as the EI is a random value and associated with the local optima (See Eq. (2)). Then the response at the  $\mathbf{P}_1$  is calculated by the cost function and the number of sampling points is updated to  $m = m + 1$ .

The second new sampling point  $\mathbf{P}_2$  is the location at the optimal output of the RBF network. This is obviously a local search. Then the response at the  $\mathbf{P}_2$  is evaluated and the number of sampling points is updated to  $m = m + 1$ .

If the terminal criterion that the number of function evaluations reaches a given  $m_{\max}$  is met, the algorithm is terminated. Otherwise, a density function  $D(\mathbf{x})$  will be constructed. The third new sampling point  $\mathbf{P}_3$  which located in the sparse region is the global minimum of the density function. This is helpful to the global search. Then, the value of  $m$  is updated for the next iteration as shown in Fig. 2.



**Figure 2.** The flow chart of the HSM-based EGO algorithm.

## 4. NUMERICAL EXAMPLES

In this section, the validity of our algorithm will be demonstrated with the examples of a test function and a transmitting antenna design.

### 4.1. A Test Function

We consider the following problem

$$f(\mathbf{x}) = \frac{1}{2} \sum_{i=1}^k (x_i^4 - 16x_i^2 + 5x_i) \rightarrow \min \quad (-5 \leq x_i \leq 5), \quad (11)$$

where  $\mathbf{x}_G = (-2.9035, -2.9035, \dots, -2.9035)_{1 \times k}$  is the global minimum. In this example, the number of design variables  $k$  is set as 10, and the objective function at  $\mathbf{x}_G$  is  $f(\mathbf{x}_G) = -391.661$ . We apply our algorithm to find the global minimum. The number of the initial sampling points which are generated randomly is 25 (in order to compare with the results in the literature [30], we do not use OA to generate them). The maximum number of function evaluations  $m_{\max}$  is set as 150, and we obtain the average global minimum of  $-389.7621$  in 10 trials. The average convergence rate is shown in Fig. 3. In contrast, the PSO needs 10,000 evaluations to converge to an average of  $-388.832$  in 10 trials [30], and the sequential approximate optimization (SAO) needs 500 evaluations to converge to an average of  $-384.089$  in 10 trials [30].

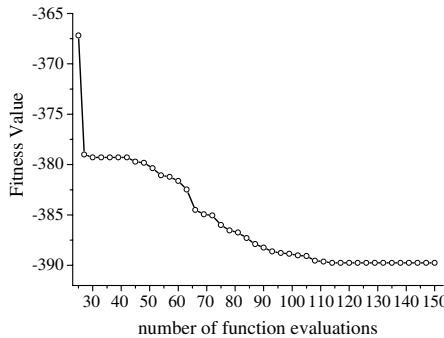


**Figure 3.** Average convergence rate for 10-D Equation (11).

### 4.2. Optimization of a Combined-Oscillator Antenna

A transmitting antenna, named combined-oscillator (CO), was designed for launching a transient pulse in the literature [31]. The

geometry of the CO antenna is shown in Fig. 4. This antenna presents a combination of electrical and magnetic oscillators which can help to expand the matching band into the low-frequency region in the limited volume of antenna. It has the voltage standing-wave ratio (VSWR) less than 4 from 100 MHz to 1200 MHz (Fig. 5), an asymmetric power pattern in the meridional plane with an up-shift of  $15^\circ$  (Fig. 6), and a symmetrical power pattern in the azimuthal plane with the cardiac type (Fig. 7). This antenna has been used as a steering antenna array element that radiates the ultra-wideband electromagnetic pulse [31, 34].

The HSM-based EGO algorithm is applied to optimize the VSWR and normalized power pattern [35] of the CO antenna. The number of the design variables is twelve, and their ranges are listed in Table 1. Other parameters shown in Fig. 4 are set as constants.

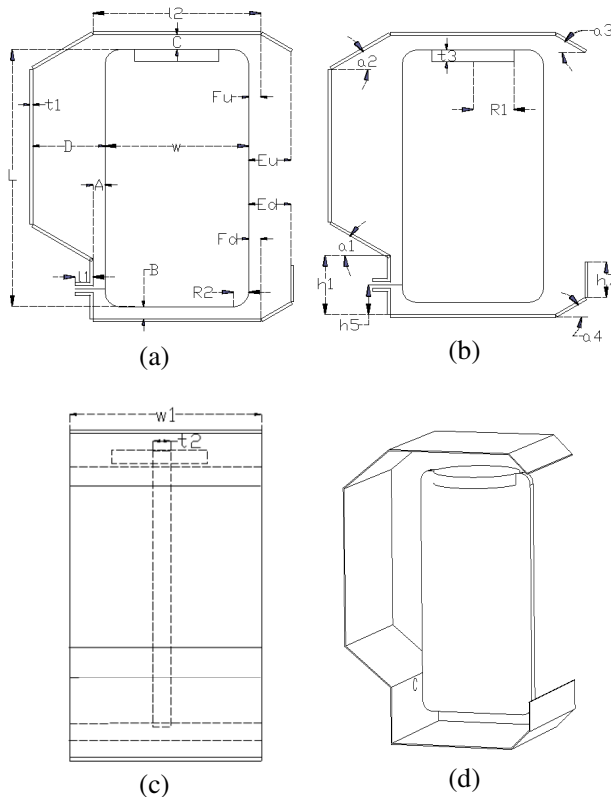


**Figure 4.** The geometry of the CO antenna: (a) side view, (b) side view, (c) back view, (d) 3D view.

**Table 1.** Design parameters for the CO antenna (unit: mm).

design parameter	$A$	$B$	$C$	$D$	$E$ ( $E_u=E_d$ )	$F$ ( $F_u=F_d$ )
lower bound	15	20	20	60	30	0
upper bound	30	60	60	200	50	20
design parameter	$w$	$w1$	$a3$	$a4$	$h7$	$t2$
lower bound	100	200	30	30	0	10
upper bound	250	500	60	60	50	20

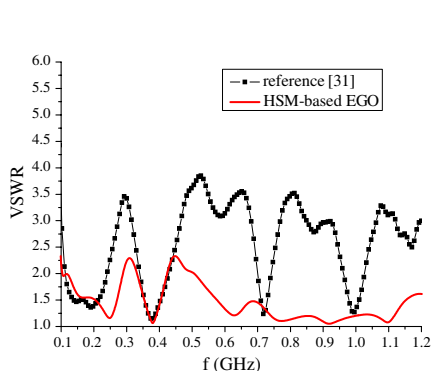


**Figure 5.** The Comparison of the VSWR given in [31] and the one obtained by the HSM-based EGO algorithm.

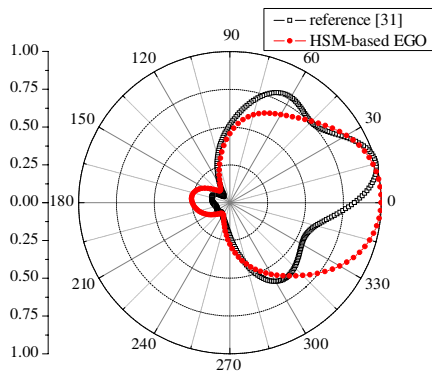


**Figure 6.** The Comparison of the normalized power pattern in the meridional plane given in [31] and the one obtained by the HSM-based EGO algorithm.

The design problem is defined as the minimization of the objective function

$$F(\mathbf{x}) = offset[mld(\mathbf{x})] + \max\{vswr(\mathbf{x}, f), f \in [100 \text{ MHz}, 1200 \text{ MHz}]\}, \tag{12}$$

where  $\mathbf{x} = \{A, B, C, D, E, F, w, w1, a3, a4, h7, t2\}$ ,  $mld(\mathbf{x})$  is the main lobe direction of the power pattern in the meridional plane for  $\mathbf{x}$ . If  $mld(\mathbf{x}) \in [0, 10] \text{ or } [350, 360]$ ,  $offset(z) = 0$ , otherwise  $offset(z) = z$ .

The number of initial sampling points which were determined by OA is 27, and the maximum number of function evaluations  $m_{\max}$  in our algorithm is set as 200.

The optimal solution obtained by our algorithm is recorded in Table 2. As shown in Fig. 5 and Fig. 6, the VSWR is improved dramatically in the bandwidth ranging from 100 MHz to 1200 MHz, while the main lobe direction of the power pattern in the meridional

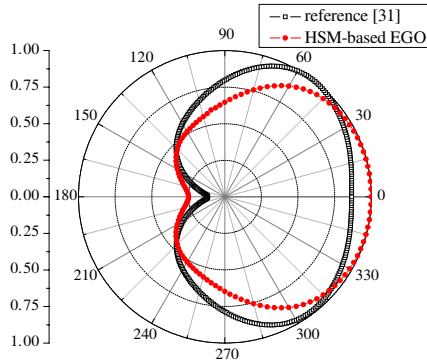


**Figure 7.** The Comparison of the normalized power pattern in the azimuthal plane given in [31] and the one obtained by the HSM-based EGO algorithm.

plane is  $0^\circ$  compared with  $15^\circ$  given in [31]. It is shown in Fig. 7 that the main lobe of the power pattern in the azimuthal plane is narrower. These improvements are very useful for the application of antenna in the array.

#### 4.3. Comparisons of the HSM-based EGO, GA-based EGO and DES Algorithms

In order to show the performance of our algorithm, we also apply the GA-based EGO and the DES algorithms to optimize the same CO antenna respectively.

The initial set of the GA-based EGO is the same as the HSM-based EGO algorithm. Furthermore, the maximum number of iterations in the GA-based EGO algorithm is set as 300.

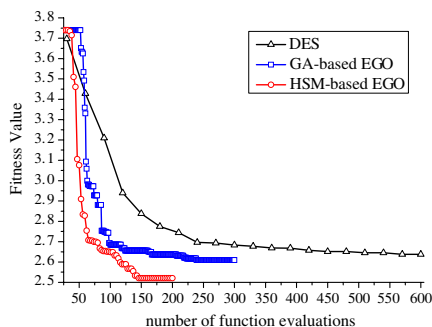
The population size of the DES algorithm is set as 30 and its maximum number of iterations set as 20. Thus, there are total 600 function evaluations for the DES algorithm in this optimization.

Table 2 shows the best solutions obtained by these three algorithms in 10 independent runs. The average convergence rates for them are shown in Fig. 8. It is worth stressing that the optimization time is dominated by the function evaluation — the numerical simulation of the CO antenna by the electromagnetic solver in this example. Therefore the performance of algorithm can be indicated by the number of function evaluations.

It can be seen from Fig. 8 that the capabilities of our algorithm both in the fast convergence and the global search are superior to those of the GA-based EGO and DES algorithms in this 12-dimensional

**Table 2.** Optimal parameters for the CO antenna obtained by different algorithms (unit: mm).

Design Parameter	<i>A</i>	<i>B</i>	<i>C</i>	<i>D</i>	<i>E</i>	<i>F</i>
HSM-based EGO	15.0	52.3	59.6	200.0	30.0	15.5
GA-based EGO	15.0	60.0	59.8	200.0	35.7	10.0
DES	15.0	43.3	59.3	199.5	30.3	10.2
Design Parameter	<i>w</i>	<i>w1</i>	<i>a3</i>	<i>a4</i>	<i>h7</i>	<i>t2</i>
HSM-based EGO	240.0	417.6	50.3	49.7	30.3	20.0
GA-based EGO	143.8	325.5	44.2	25.5	30.5	20.0
DES	209.4	331.1	52.4	50.7	38.6	13.6



**Figure 8.** Comparisons of the average convergence rates by the different algorithms.

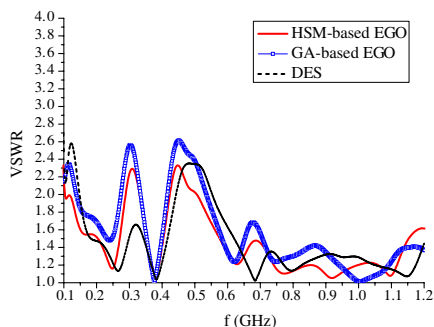


**Figure 9.** Comparisons of the VSWR by the different algorithms.

optimization. The fitness value of the HSM-based EGO algorithm converges to 2.52 with 200 function evaluations, while the fitness values of the GA-base EGO and DES algorithms are about 2.6 with 300 and 600 function evaluations respectively. In our simulations, the electromagnetic solver CST MWS is employed and run on the ASUS server with 4 cores, CPU: Xeon X3330 @ 2.66 GHz. The average calculation time for the optimization are about 67 hours, 100 hours and 200 hours for the HSM-based EGO, GA-based EGO and DES algorithms respectively.

The VSWR and power patterns of the best solutions obtained by these three algorithms are presented in Fig. 9–Fig. 11. We can see that their comprehensive performances are comparable. These comparisons show that our algorithm is very efficient in dealing with the high-dimensional antenna design problems.

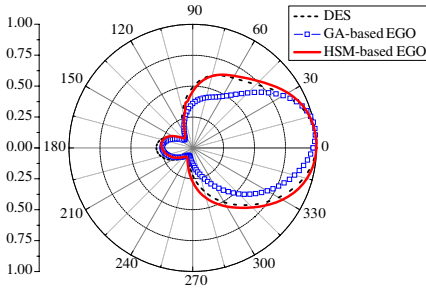


**Figure 10.** Comparisons of the normalized power patterns in the meridional plane by the different algorithms.

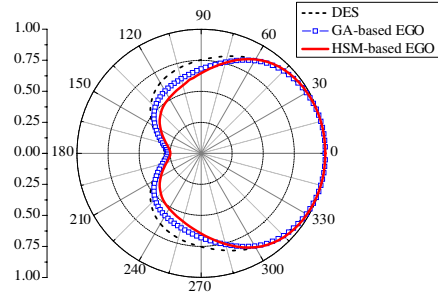


**Figure 11.** Comparisons of the normalized power patterns in the azimuthal plane by the different algorithms.

## 5. CONCLUSION

In this paper, we propose a HSM-based EGO algorithm for the high-dimensional antenna optimization. We introduce a sampling strategy implemented by the hybrid surrogate models into EGO algorithm. Numerical examples show that the global optimum can be found in a small number of function evaluations. Compared with the GA-based EGO and DES algorithms, our algorithm obtains better results of the convergence rate. It is shown that the design methodology is an effective way for the high-dimensional antenna optimization.

## ACKNOWLEDGMENT

This work was supported by the NSAF of China (Grant No. 11076022), the Open Research Fund of Key Laboratory of Cognitive Radio and Information Processing of Ministry of Education of China, and the Fund of Key Laboratory of High Power Microwave Technology.

## REFERENCES

1. Jones, D. R., M. Schonlau, and W. J. Welch, "Efficient global optimization of expensive black-box functions," *Journal of Global Optimization*, Vol. 13, No. 4, 455–492, 1998.
2. Siakavara, K., "Novel fractal antenna arrays for satellite networks: Circular ring Sierpinski carpet arrays optimized by genetic algorithms," *Progress In Electromagnetics Research*, Vol. 103, 115–138, 2010.

3. Reza, A. W., M. S. Sarker, and K. Dimyati, "A novel integrated mathematical approach of ray-tracing and genetic algorithm for optimizing indoor wireless coverage," *Progress In Electromagnetics Research*, Vol. 110, 147–162, 2010.
4. Dadgarnia, A. and A. A. Heidari, "A fast systematic approach for microstrip antenna design and optimization using ANFIS and GA," *Journal of Electromagnetic Waves and Applications*, Vol. 24, No. 16, 2207–2221, 2010.
5. Xu, O., "Collimation lens design using AI-GA technique for gaussian radiators with arbitrary aperture field distribution," *Journal of Electromagnetic Waves and Applications*, Vol. 25, No. 5–6, 743–754, 2011.
6. Zaharis, Z. D. and T. V. Yioultis, "A novel adaptive beamforming technique applied on linear antenna arrays using adaptive mutated boolean PSO," *Progress In Electromagnetics Research*, Vol. 117, 165–179, 2011.
7. Deligkaris, K. V., Z. D. Zaharis, D. G. Kampitaki, S. K. Goudos, I. T. Rekanos, and M. N. Spasos, "Thinned planar array design using boolean PSO with velocity mutation," *IEEE Transactions on Magnetics*, Vol. 45, No. 3, 1490–1493, 2009.
8. Chamaani, S., S. A. Mirtaheri, M. Teshnehlab, M. A. Shooredeli, and V. Seydi, "Modified multi-objective particle swarm optimization for electromagnetic absorber design," *Progress In Electromagnetics Research*, Vol. 79, 353–366, 2008.
9. Goudos, S. K., Z. D. Zaharis, D. G. Kampitaki, I. T. Rekanos, and C. S. Hilas, "Pareto optimal design of dual-band base station antenna arrays using multi-objective particle swarm optimization with fitness sharing," *IEEE Transactions on Magnetics*, Vol. 45, No. 3, 1522–1525, 2009.
10. Liu, D., Q. Feng, W.-B. Wang, and X. Yu, "Synthesis of unequally spaced antenna arrays by using inheritance learning particle swarm optimization," *Progress In Electromagnetics Research*, Vol. 118, 205–221, 2011.
11. Wang, W.-B., Q. Feng, and D. Liu, "Application of chaotic particle swarm optimization algorithm to pattern synthesis of antenna arrays," *Progress In Electromagnetics Research*, Vol. 115, 173–189, 2011.
12. Goudos, S. K., et al., "Application of a comprehensive learning particle swarm optimizer to unequally spaced linear array synthesis with side lobe level suppression and null control," *IEEE Antennas and Wireless Propagation Letters*, Vol. 9, 125–129, 2010.

13. Carro Ceballos, P. L., J. de Mingo Sanz, and P. G. Dúcar, "Radiation pattern synthesis for maximum mean effective gain with spherical wave expansions and particle swarm techniques," *Progress In Electromagnetics Research*, Vol. 103, 355–370, 2010.
14. Zaharis, Z. D., S. K. Goudos, and T. V. Yioultis, "Application of boolean PSO with adaptive velocity mutation to the design of optimal linear antenna arrays excited by uniform amplitude current distribution," *Journal of Electromagnetic Waves and Applications*, Vol. 25, No. 10, 1422–1436, 2011.
15. Storn, R. and K. Price, "Differential evolution — A simple and efficient heuristic for global optimization over continuous spaces," *Journal of Global Optimization*, Vol. 11, No. 4, 341–359, 1997.
16. Goudos, S. K., Z. D. Zaharis, and T. V. Yioultis, "Application of a differential evolution algorithm with strategy adaptation to the design of multi-band microwave filters for wireless communications," *Progress In Electromagnetics Research*, Vol. 109, 123–137, 2010.
17. Goudos, S. K., K. Siakavara, E. Vafiadis, and J. N. Sahalos, "Pareto optimal Yagi-Uda antenna design using multi-objective differential evolution," *Progress In Electromagnetics Research*, Vol. 105, 231–251, 2010.
18. Xie, L., Y. C. Jiao, Y. Q. Wei, and G. Zhao, "A compact band-notched UWB antenna optimized by a novel self-adaptive differential evolution algorithm," *Journal of Electromagnetic Waves and Applications*, Vol. 24, No. 17–18, 2353–2361, 2010.
19. Dib, N. I., S. K. Goudos, and H. Muhsen, "Application of Taguchi's optimization method and self-adaptive differential evolution to the synthesis of linear antenna arrays," *Progress In Electromagnetics Research*, Vol. 102, 159–180, 2010.
20. Li, R., L. Xu, X. W. Shi, N. Zhang, and Z. Q. Lv, "Improved differential evolution strategy for antenna array pattern synthesis problems," *Progress In Electromagnetics Research*, Vol. 113, 429–441, 2011.
21. Li, F., Y. C. Jiao, L. S. Ren, Y. Y. Chen, and L. Zhang, "Pattern synthesis of concentric ring array antennas by differential evolution algorithm," *Journal of Electromagnetic Waves and Applications*, Vol. 25, No. 2–3, 421–430, 2011.
22. Southall, H. L., T. H. O'Donnell, and B. Kaanta, "Endgame implementations for the efficient global optimization (EGO) algorithm," *Proceedings of SPIE — The International Society for Optical Engineering: Evolutionary and Bio-Inspired Computation: Theory and Applications III*, Vol. 7347, 73470Q, 2009.

23. Southall, H. L., T. H. O'Donnell, and J. S. Derov, "Optimum design of antennas using metamaterials with the efficient global optimization (EGO) algorithm," *Proceedings of SPIE — The International Society for Optical Engineering: Evolutionary and Bio-Inspired Computation: Theory and Applications IV*, Vol. 7704, 770408, 2010.
24. Southall, H. L., T. H. O'Donnell, and B. Kaanta, "Efficient global optimization for antenna design," *Proceedings of the 2008 Antenna Applications Symposium*, 250–269, 2008.
25. O'Donnell, T. H., H. L. Southall, and B. Kaanta, "Efficient global optimization for a limited parameter antenna design," *Proceedings of SPIE — The International Society for Optical Engineering: Evolutionary and Bio-Inspired Computation: Theory and Applications II*, Vol. 6964, 69640J, 2008.
26. Sheng, N., C. Liao, W. Lin, L. Chang, Q. Zhang, and H. Zhou, "A hybrid optimized algorithm based on ego and Taguchi's method for solving expensive evaluation problems of antenna design," *Progress In Electromagnetics Research C*, Vol. 17, 181–192, 2010.
27. O'Donnell, T. H., H. Southall, S. Santarelli, and H. Steyskal, "Applying EGO to large dimensional optimizations: A wideband fragmented patch example," *Proceedings of SPIE — The International Society for Optical Engineering: Evolutionary and Bio-Inspired Computation: Theory and Applications IV*, Vol. 7704, 770407, 2010.
28. Huang, D., T. T. Allen, W. I. Notz, and N. Zeng, "Global optimization of stochastic black-box systems via sequential Kriging meta-models," *Journal of Global Optimization*, Vol. 34, No. 3, 441–466, 2006.
29. Sharif, B., G. G. Wang, and T. Y. Elmeekawy, "Mode pursuing sampling method for discrete variable optimization on expensive black-box functions," *Journal of Mechanical Design, Transactions of the ASME*, Vol. 130, No. 2, 021402, 2008.
30. Kitayama, S., M. Arakawa, and K. Yamazaki, "Sequential approximate optimization using radial basis function network for engineering optimization," *Optimization and Engineering*, Vol. 12, No. 4, 535–557, 2011.
31. Wang, J. G., C. M. Tian, H. F. Xia, and D. B. Ge, "Numerical simulations on radiation properties of combined-oscillator antenna," *High Power Laser and Particle Beams*, Vol. 17, No. 4, 581–585, 2005.
32. Simpson, T. W., J. D. Poplinski, P. N. Koch, and J. K. Allen, "Metamodels for computer-based engineering design: Survey and

- recommendations,” *Engineering with Computers*, Vol. 17, No. 2, 129–150, 2001.
33. Chen, S., C. F. N. Cowan, and P. M. Grant, “Orthogonal least squares learning algorithm for radial basis function networks,” *IEEE Transactions on Neural Networks*, Vol. 2, No. 2, 302–309, 1991.
  34. Wang, J. G., C. M. Tian, H. F. Xia, and D. B. Ge, “Numerical simulation of combined oscillator antenna array,” *High Power Laser and Particle Beams*, Vol. 18, No. 7, 1144–1148, 2006.
  35. Allen, O. E., D. A. Hill, and A. R. Ondrejka, “Time-domain antenna characterizations,” *IEEE Transactions on Electromagnetic Compatibility*, Vol. 35, No. 3, 339–345, 1993.